# Spin scattering by dislocations in III-V semiconductors

Debdeep Jena*
*Department of Electrical Engineering, University of Notre Dame, Notre Dame, Indiana 46556, USA*
(Received 18 June 2004; revised manuscript received 20 September 2004; published 3 December 2004)

A semiclassical treatment of spin relaxation in direct-gap compound semiconductors due to scattering by edge dislocations from both charged cores, and the strain fields surrounding them is presented. The results indicate a deleterious effect on spin transport in narrow bandgap III-V semiconductors due to dislocation scattering. However, this form of scattering is found to be surprisingly benign for wide-bandgap semiconductors with small spin-orbit coupling (such as GaN). This observation leads to a proposal for possible lattice-mismatched hybrid heterostructure devices that take advantage of the long spin lifetimes of the wide-bandgap semiconductors for transporting spin over large distances acting as spin-interconnects, and the wide tunability of spin in the narrow-bandgap semiconductors for spin logic operations.

DOI: 10.1103/PhysRevB.70.245203 PACS number(s): 81.10.Bk, 72.80.Ey

## I. INTRODUCTION

The list of proposed semiconductor-based spintronic devices starting with the Datta-Das spin field-effect transistor (FET)[1] rely on two competing requirements, provided that spin polarized carriers can be efficiently injected into the channel.[2] First, one needs to be able to controllably flip the spin of a population of injected polarized carriers in the channel. Second, impurity and defect scattering that occurs in the spin FET channel should not cause complete spin relaxation. This is necessary, so that spin polarization of the carriers is controlled exclusively by the electric field applied by the gate voltage (by the Rashba effect). Strong spin control is achieved in narrow bandgap semiconductors such as InAs (or the alloy InGaAs) due to the large spin-orbit (SO) splitting in these materials. However, due to the very same reason, spin scattering is also enhanced; scattering from the variations in the electric potential due to impurities and defects is just as effective in randomizing the spin.

One approach to address these contradictory requirements is to use a narrow bandgap semiconductor for spin manipulation, and a wide-bandgap semiconductor for spin transport. The relative advantages of a wide-bandgap semiconductor (with low SO splitting) for spin transport was studied by Krishnamurthy *et al.* in their recent work.[3] They compared the spin transport properties in GaN and GaAs. They find that the spin lifetimes in GaN can be up to three orders of magnitude longer than in GaAs at all temperatures, and predict a room-temperature spin mean-free path of $\sim$1 cm for high-purity GaN (i.e., without dislocations). Such high spin mean-free paths would make the wide bandgap semiconductor ideal for communication of spin states between spin FET's separated by macroscopic distances, akin to global interconnects in integrated circuits.

Having narrow and wide bandgap semiconductor layers in the same structure calls for lattice-mismatched epitaxy. This will result in the formation of dislocations upon growth of bulk layers, as is observed upon growth of semiconductors for which no lattice matched substrates are currently available. How harmful are dislocations for spin transport? This topic is investigated in this work using a semiclassical approach.

## II. THEORETICAL FORMALISM

The effect of various defects and scattering sources on spin relaxation has been studied previously. Scattering from ionized impurities, and optical and acoustic phonons have been used to explain the spin relaxation rates in various semiconductors.[4,5] However, the effect of dislocations on spin transport in semiconductors has not received much attention. Spin relaxation by dislocation scattering has been investigated by Zholkievskii *et al.* for metals[6] with a strong spin-orbit coupling, and by Stroud *et al.* for hybrid II-VI/III-V heterostructures for electrical spin injection.[7] Beschoten *et al.* have performed an experimental study[8] of the spin relaxation time in doped GaN. They qualitatively suggest that dislocation scattering is a benign process for spin scattering. However, due to the lack of theoretical analysis of spin scattering due to dislocations, no quantitative analysis was presented. This work presents a semiclassical analysis of the effect of dislocations on spin transport, and points out how the results are useful in light of the discussion of the hybrid spin FET architecture proposed. The results show that the experimental room-temperature spin-scattering rate measured in GaN may be explained by invoking dislocation scattering.

This work concentrates on conduction electron spin relaxation by dislocation scattering due to the precessional D'Yakonov-Perel' (DP) mechanism and by the Elliot-Yafet (EY) mechanisms due to spin-orbit interaction with the host lattice in *n*-type direct-bandgap semiconductor crystals. The Bir-Aronov-Pikus mechanism for spin relaxation, which is important in *p*-type crystals, the weak nuclear hyperfine interaction mechanism, and relaxation by the exchange-interaction with magnetic impurities are not considered here.[4] The treatment is strictly valid for cubic crystals. In that aspect, the results are strictly valid for cubic GaN, and must be modified for the more common wurtzite form of the crystal. Note that with the above assumption, spin-scattering due to dislocations becomes linked to momentum scattering.

Fermi's Golden Rule for transition rate from state $|\mathbf{k}\rangle \rightarrow |\mathbf{k}'\rangle$ by a scattering potential $V$ is

 

$$S(\mathbf{k},\mathbf{k}') = \frac{2\pi}{\hbar}|\langle \mathbf{k}|V|\mathbf{k}'\rangle|^2 \delta(\varepsilon_{\mathbf{k}} - \varepsilon_{\mathbf{k}'}). \quad (1)$$

One can define a generalized scattering rate for functions of the state $|\mathbf{k}\rangle$ as

$$\frac{1}{\tau_n(\mathbf{k})} = \sum_{\mathbf{k}'} S(\mathbf{k},\mathbf{k}')[1 - P_n(\cos\theta)], \quad (2)$$

where $P_n(x)$ is the $n$th order Legendre polynomial. For $n=1$, $P_1(\cos\theta)=\cos\theta$ and thus $1/\tau_1(\mathbf{k})$ is the momentum scattering rate, and for $n=0$, one recovers the quantum scattering rate $1/\tau_0(\mathbf{k})=\Sigma_{k'}S(\mathbf{k},\mathbf{k}')$. However, if the scattering process involves the change of a *function* of a polynomial power $|\mathbf{k}|^n$, the scattering rate gets weighted by the $n$th order Legendre polynomial factor. This distinction will be essential in evaluating scattering rates by the EY and DP mechanisms. Furthermore, this distinguishes momentum (and hence spin) scattering rates by ionized impurities and dislocations, since dislocation scattering is inherently more *anisotropic*[9,10] due to its spatially extended nature.

The conduction band Hamiltonian in the effective mass approximation for a direct-gap semiconductor around the $\Gamma$ point in the Brillouin zone may be written as[11]

$$H_c = \frac{\hbar^2 k^2}{2m_c} + \tfrac{1}{2}\alpha_c \frac{\hbar^3}{\sqrt{2m_c^3 E_g}}(\boldsymbol{\kappa}\cdot\boldsymbol{\sigma}) + \tfrac{1}{2}C_3(\boldsymbol{\sigma}\cdot\boldsymbol{\varphi}) + W, \quad (3)$$

where $\sigma$ are the Pauli spin matrices, $\kappa_x = k_x(k_y^2 - k_z^2)$ (other terms by cyclic permutation), $\alpha_c = (4m_c/3m_0)\eta(1-\eta/3)^{-1/2}$, $C_3$ is related to the conduction band deformation potential, and $\varphi_z = \epsilon_{zx}k_x - \epsilon_{zy}k_y$ (other terms by cyclic permutation). The (direct) bandgap is $E_g$, the valence band spin orbit splitting is $\Delta$, and $\eta = \Delta/(\Delta + E_g)$. Also, $m_c$ is the conduction band effective mass (at the $\Gamma$ point), $m_0$ is the free electron mass, $\hbar k_i$ is the electron quasimomentum along the $i$ direction, and $\epsilon_{ij}$ are strain components. $W$ is the perturbation potential.

The second term in the Hamiltonian depicts the $k^3$ Dresselhaus spin splitting of the conduction band in the absence of inversion symmetry,[12] and the third term depicts the modification of electron energy spectrum in the presence of uniaxial strain. This work is concerned with dilute concentrations of dislocations, whose localized strain fields are assumed to cause negligible change to the crystal energy spectrum. Furthermore, it is assumed that the lattice-mismatched layer has relaxed completely by the formation of dislocations. So the third term in the Hamiltonian is neglected in the analysis, and the dislocation potential is treated as a perturbation to the Hamiltonian of the first two terms, resulting in spin scattering.

### A. Eliott-Yafet scattering

The perturbation potential may be split into two parts ($W = V_{\text{direct}} + V_{\text{SO}}$)—one arising from the direct potential of the perturbation, and the second due to the spin-orbit interaction. It is now well established that spin-orbit interaction of electrons results in the mixing of the spin states in the eigenfunctions of the crystal Hamiltonian. As a result, for semiconductors, spin is scattered much more strongly by the direct perturbation potential than the spin-orbit part associated with it. This was first pointed out by Elliott[13] and Yafet,[14] and is now known as the Elliott-Yafet (EY) scattering mechanism.

The problem of finding the scattering rate thus hinges on finding the matrix elements $\langle \mathbf{k}\uparrow|V_{\text{direct}}|\mathbf{k}'\downarrow\rangle$, and summing them over all available states via the application of Fermi's Golden rule of scattering rates. In this formalism, the spin scattering rate is naturally linked with the momentum scattering rate; a certain fraction of momentum scattering events result in spin flip. It has been shown by Chazalviel[15] that the relation between the spin scattering rate $1/\tau_s^{\text{EY}}(\mathbf{k})$ and momentum scattering rate $1/\tau_1(\mathbf{k})$ for the EY mechanism is

$$\frac{1}{\tau_s^{\text{EY}}(k)} = \frac{1}{\tau_1(k)}\frac{4\Gamma}{3}\left(\frac{\varepsilon(\mathbf{k})}{E_g}\right)^2 \Phi, \quad (4)$$

where $\varepsilon(\mathbf{k})$ is the electron energy, $E_g$ the bandgap,

$$\Gamma = \left(\frac{2\eta}{3}\frac{1-\eta/2}{1-\eta/3}\right)^2, \quad (5)$$

and the factor $\Phi$ is given by[16]

$$\Phi = \frac{\int_{-1}^{+1} d\mu(1-\mu^2)\sigma(\mu)}{\int_{-1}^{+1} d\mu(1-\mu)\sigma(\mu)}. \quad (6)$$

Here, $\mu=\cos\theta$, $\theta$ being the angle of scattering; for elastic scattering, the relation $\cos\theta = \mathbf{k}\cdot\mathbf{k}'/|\mathbf{k}|^2$ holds. $\sigma(\cos\theta)$ is the scattering cross section, which is proportional to the scattering matrix element $\sigma(\cos\theta) \propto |\langle \mathbf{k}|V_{\text{direct}}|\mathbf{k}'\rangle|^2$. Note that for dislocations, it is preferable to define a scattering "diameter" rather than a scattering "cross section" due to the linear nature of the defect; however, the proportionality still holds, thus enabling the evaluation of $\Phi$ once the effective matrix element is known.

### B. Dyakonov-Perel scattering

In the absence of inversion symmetry, the conduction band energy eigenvalues are spin-split at every quasimomenta value $\hbar\mathbf{k}$ into $\hbar^2|\mathbf{k}|^2/2m_c \pm \eta|\kappa|$, according to the second Dresselhaus term in the Hamiltonian. However, the spin splitting $\Delta\varepsilon_{\mathbf{k}} = 2\eta|\kappa|$ is much smaller than typical carrier energies ($\Delta\varepsilon_{\mathbf{k}} \sim kT/300$ for $\varepsilon_{\mathbf{k}} \sim kT$ at $T=300$ K). Thus, this splitting is treated as the perturbation potential leading to spin scattering. The electron spin precesses about the vector $\kappa$, which is perpendicular to the electron quasimomentum direction $\mathbf{k}/|\mathbf{k}|$. With each momentum scattering, the precession axis changes irreversibly, and precession starts anew, leading to a diffusive spreading of electron spin direction. The more frequent the momentum scattering, the less time the spin has to change from its initial precession axis; thus, in this form of scattering, spin relaxation time is *inversely* proportional to the momentum scattering time. This method of spin relaxation was first recognized by D'Yakonov and Perel[17] (it is referred to as DP scattering).

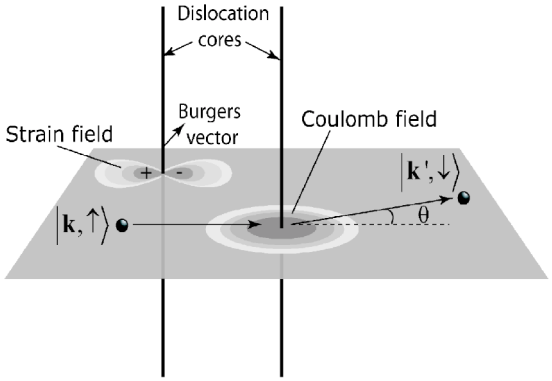


FIG. 1. The strain and Coulomb fields around edge dislocations that cause spin scattering are shown schematically. Without screening by free carriers, the strain field follows a $\sin\varphi/r$ dependence from the dislocation core, and the Coulomb field follows a $1/r$ dependence.

By decomposing the components of the vector $\kappa=k_x(k_y^2-k_z^2)\mathbf{x}+k_y(k_z^2-k_x^2)\mathbf{y}+k_z(k_x^2-k_y^2)\mathbf{y}$ into spherical coordinates, and carrying out a spherical unweighted average, one obtains for a parabolic energy dispersion $\kappa_i^2=4k^6/105=32m_c^3\varepsilon(k)^3/105\hbar^6$. D'Yakonov and Perel have shown in their seminal work[17] by using the time-evolution property of spin density matrices that the spin-relaxation rate is then given by

$$\frac{1}{\tau_s^{\mathrm{DP}}(k)}=\Omega_0^2\tau_3(k), \tag{7}$$

where $\Omega_0^2=(32/105)\alpha_c^2[\varepsilon(k)^3/\hbar^2E_g]$. Since the precessional spin relaxation rate depends on the rate of dephasing of $\kappa\sim k^3$ instead of $k$, the weighting factor for spin relaxation rate becomes $1-P_3(\cos\theta)$. Since *momentum* scattering rates are usually known from electrical transport theory, it is useful to relate the two rates by introducing a new factor

$$\frac{1/\tau_3(\mathbf{k})}{1/\tau_1(\mathbf{k})}=\gamma_3(\mathbf{k})=\frac{\int_{-1}^{+1}d\mu[1-P_3(\mu)]\sigma(\mu)}{\int_{-1}^{+1}d\mu[1-P_1(\mu)]\sigma(\mu)}. \tag{8}$$

## III. TWO DISLOCATION POTENTIALS

In this work, edge dislocations are considered exclusively. The case for screw dislocations can be treated using a similar formalism with the corresponding scattering potentials. The crystal lattice around an edge dislocation is strained, leading to a scattering potential for electrons. Similarly, the core of the dislocation has a line of dangling bonds, which donate or accept electrons from the host lattice, and get charged. As a result, the dislocation becomes a line charge, and the Coulombic potential leads to scattering of electrons moving in the conduction band. Both these potentials are schematically shown in Fig. 1. In the following, the spin scattering rates due to the two dislocation related potentials are calculated.

### A. Dislocation strain fields

Since the bandgap of the semiconductor depends on the strain via the deformation potential, the variation of the conduction/valence band extrema around the dislocation follows the strain fields. The deviation of conduction band-edge from flat-band conditions around an edge dislocation is[18,19]

$$V_{\mathrm{st}}(r)=-\frac{a_C^\star b_e}{2\pi}\frac{\sin\varphi}{r}, \tag{9}$$

where $a_C^\star=a_C[(1-2\sigma)/(1-\sigma)]$, $a_C$ is the conduction band deformation potential, $\sigma$ is the Poisson ratio of the crystal, and $b_e=|\mathbf{b_e}|$ is the length of the Burgers vector. $r=|\mathbf{r}|$ is the radial distance from the dislocation core, and $\varphi$ is the angle between $\mathbf{r}$ and the Burgers vector $\mathbf{b}_e$. Note that upon scattering, the electron quasimomentum component $\hbar\mathbf{k}_\perp$ is changed only; the dislocation does not change the parallel component owing to the translational invariance of the dislocation potential along its axis. Long-range variations from flat-band conditions in semiconductors are screened by mobile carriers. The characteristic screening length of long-range potentials is the Debye screening length for non-degenerate carriers, and the Thomas-Fermi length for degenerate carrier densities. For now, the screening length $\lambda$ is retained as a parameter to be evaluated for different regimes.

The square of the screened momentum matrix element (with screening length $\lambda$) is given by

$$|\widetilde{V}_{\mathrm{st}}(q)|^2=\frac{(a_C^\star)^2b_e^2}{8\pi^2}\frac{\lambda^2}{1+(q\lambda)^2}, \tag{10}$$

where the scattering is from state $|\mathbf{k}\rangle\rightarrow|\mathbf{k}+\mathbf{q}\rangle$. Note that this is evaluated by an angle-averaging over various randomly oriented Burgers vectors for different dislocations.[19] By summing the scattering rates over all possible final $k$ states, the *exact* momentum scattering rate is

$$\frac{1}{\tau_1^{\mathrm{st}}(k)}=\frac{N_{\mathrm{disl}}m_cb_e^2(a_C^\star)^2}{2\hbar^3}\frac{y-1}{k^2y}, \tag{11}$$

where $N_{\mathrm{disl}}$ is the areal dislocation density, $x=k\lambda$, and $y=\sqrt{1+2x^2}$.

For the EY mechanism, the factor $\Phi_{\mathrm{st}}$ has an asymptotic value $\Phi_{\mathrm{st}}(x\rightarrow\infty)=1$. Similarly, the factor $\gamma_3$ for DP scattering has an asymptotic behavior $\gamma_{\mathrm{st}}(x\rightarrow\infty)=9/4$. The asymptotic values are important, since the first Born approximation from which Fermi's Golden Rule is derived requires that $2(k\lambda)^2\gg1$; this holds in general in the degenerate and nondegenerate limits.[15] The exact formulas of the two factors appear in the Appendix.

### B. Dislocation charge

If the dislocation is considered a line charge with charge density $e/c$ C m$^{-1}$, then the screened potential surrounding the dislocation is given by[20,21]

$$V_{\mathrm{ch}}(r)=\frac{e}{2\pi\epsilon_sc}K_0\left(\frac{r}{\lambda}\right), \tag{12}$$

where $K_0$ is the zero-order modified Bessel function, $\epsilon_s$ is the dielectric constant of the host semiconductor, and $\lambda$ is the

screening length. The same screening length as used for scattering from strain fields appears for charged dislocation scattering. This is justified since both unscreened potentials have a characteristic $1/r$ long-range variation, which results in similar screening.

The squared scattering matrix element thus becomes[22]

$$|\widetilde{V}_{\rm ch}(q)|^2 = \left(\frac{e^2}{\epsilon_s c}\right)^2 \left(\frac{\lambda^2}{1+(q\lambda)^2}\right)^2, \tag{13}$$

and leads to a momentum scattering time[10]

$$\frac{1}{\tau_1^{\rm ch}(k)} = \frac{e^4 m^\star N_{\rm disl}}{\hbar^3 \epsilon_s^2 c^2} \frac{\lambda^4}{y^3}. \tag{14}$$

The EY factor for dislocation charge field scattering has an asymptotic behavior $\Phi_{\rm ch}(x\to\infty)=2$, and the DP factor $\gamma_{\rm ch}(x\to\infty)=6$ (from the Appendix), similar to small-angle scattering for ionized impurities.[16]

## IV. SPIN SCATTERING RATES

With the above formulation, spin scattering rates may be calculated in the case of arbitrary degeneracy of carriers, and at all temperatures, by taking the energy distribution of carriers into account. However, the most useful cases arise for the extreme cases of nondegenerate distributions and degenerate distribution of electrons. For such cases the spin scattering rates due to dislocation strain and charge fields reduce into particularly simple forms.

### A. Scattering rates in the degenerate and nondegenerate limits

In the degenerate limit, transport occurs by carriers at the Fermi level, and the scattering rates can be evaluated at the Fermi surface. As a result, the dimensionless term $k\lambda \to k_F\lambda_{\rm TF}$, where $k_F=(3\pi^2 n)^{1/3}$, $n$ being the 3D electron density and $\lambda_{\rm TF}=\sqrt{2\epsilon_s\varepsilon_F/3e^2n}$ is the Thomas-Fermi screening length. For the Born approximation to be valid, $2(k_F\lambda_{\rm TF})^2 \gg 1$, and for nominal values of electron density ($10^{16}/{\rm cm}^3 \leqslant n \leqslant 10^{20}/{\rm cm}^3$), we find $8 \leqslant 2(k_F\lambda_{\rm TF})^2 \leqslant 50$, weakly satisfying the required condition. The carrier energy is given by the Fermi energy, which is determined by the carrier density via $\varepsilon_F=\hbar^2k_F^2/2m_c$. In this aspect, the properties of the degenerate semiconductor are similar to that in a metal.

Similarly, for nondegenerate carrier distributions, the Fermi-Dirac distribution of carrier energies may be approximated by a Maxwell-Boltzmann distribution. With this approximation, $\varepsilon(\mathbf{k}) \approx kT$, and a parabolic energy dispersion is used to relate the electron quasimomentum to the temperature $\hbar k \approx \sqrt{2m_c kT}$. For finding the ensemble spin-scattering rate, energy averaging by following the prescription for a Maxwell-Boltzmann gas yields

$$\left.\frac{1}{\tau_s}\right|_{\rm ND} = \frac{\int \tau_s(\varepsilon)^{-1}\sqrt{\varepsilon}e^{-\varepsilon/kT}d\varepsilon}{\int \sqrt{\varepsilon}e^{-\varepsilon/kT}d\varepsilon}. \tag{15}$$

The screening length is the well-known Debye length given by $\lambda_D=\sqrt{\epsilon_s kT/e^2n^\star}$, where $n^\star$ is the free-carrier density effective in screening. For $n$-type doped semiconductors, the effective screening density is assumed to be the doping density for nondegenerate cases due to complete ionization.

#### 1. Eliott-Yafet scattering mechanism

The EY spin scattering rate for a degenerate ($D$) electron distribution by the strain field of the dislocation is

$$\left.\frac{1}{\tau_s^{\rm EY}}\right|_{D,{\rm str}} \approx \frac{\Gamma}{3} N_{\rm disl} b_e^2 \left(\frac{a_C^\star}{E_g}\right)^2 \frac{\varepsilon_F}{\hbar}. \tag{16}$$

The asymptotic factors evaluated earlier for $k\lambda\to\infty$, with Eqs. (4) and (11) are used here. Using the same forms for a nondegenerate (ND) electron gas, the spin scattering rate from the dislocation strain field is found to be

$$\left.\frac{1}{\tau_s^{\rm EY}}\right|_{\rm ND,str} \approx \frac{\Gamma}{2} N_{\rm disl} b_e^2 \left(\frac{a_C^\star}{E_g}\right)^2 \frac{kT}{\hbar}. \tag{17}$$

The derived formulas yield close estimates at best; the exact scattering rates for the model of dislocation potentials may be evaluated by averaging the scattering rates over the exact Fermi-Dirac carrier energy distributions.

In a similar fashion, spin scattering rates by the EY mechanism for the dislocation charge potentials for a degenerate distribution is given by

$$\left.\frac{1}{\tau_s^{\rm EY}}\right|_{D,{\rm ch}} \approx \Gamma \sqrt{\frac{128\pi^3}{27}} \frac{N_{\rm disl}\hbar^3\varepsilon_F}{(m_c c E_g)^2\sqrt{a_B^3 n}}, \tag{18}$$

where Eqs. (4) and (14) are used. For a nondegenerate distribution,

$$\left.\frac{1}{\tau_s^{\rm EY}}\right|_{\rm ND,ch} \approx \frac{16\pi\Gamma}{3} \frac{N_{\rm disl}\hbar^3 kT}{(m_c c E_g)^2\sqrt{a_B^3 n^\star}}. \tag{19}$$

Here, $a_B=4\pi\hbar^2\epsilon_s/e^2m_c$ is the effective Bohr radius of the semiconductor.

#### 2. Dyakonov-Perel scattering mechanism

The spin scattering rates due to strain fields of dislocations by the DP mechanism for a degenerate electron gas is found to be

$$\left.\frac{1}{\tau_s^{\rm DP}}\right|_{D,{\rm st}} \approx \frac{96}{35}\left[\frac{\alpha_c^2}{N_{\rm disl}b_e^2}\right]\left[\frac{\varepsilon_F^4}{\hbar E_g (a_C^\star)^2}\right], \tag{20}$$

by using Eqs. (7) and (11), and the fact that transport occurs due to carriers at the Fermi energy.

Since $\tau_s^{\rm DP}|_{\rm st} \sim \varepsilon^4$, for the nondegenerate case, a Maxwell-Boltzmann averaging of the scattering rate over carrier energies $\langle\varepsilon^4\rangle=\Gamma(11/2)/\Gamma(3/2)(kT)^4 \approx 59(kT)^4$ can be used to obtain

$$\left.\frac{1}{\tau_s^{\rm DP}}\right|_{\rm ND,st} \approx \left[\frac{162\alpha_c^2}{N_{\rm disl}b_e^2}\right]\left[\frac{(kT)^4}{\hbar E_g (a_C^\star)^2}\right]. \tag{21}$$

Similarly, for charged-core scattering from dislocation, the DP scattering rate for a degenerate electron gas is evaluated to be

TABLE I. Material properties of InAs, GaAs, and GaN.

| Material | $E_g$(300 K, eV) | $\Delta$(eV) | $a_C$(eV) | $a_0(c_0)$ Å | $\varepsilon_s$ | $m_c/m_0$ | $\sigma$ |
|---|---|---|---|---|---|---|---|
| (1) InAs | 0.4 | 0.39 | 5.1 | 6.058 | 15.2 | 0.026 | 0.35 |
| (2) GaAs | 1.4 | 0.34 | 7.2 | 5.653 | 12.9 | 0.063 | 0.31 |
| (3) GaN | 3.4 | 0.02 | 8.0 | 3.189(5.185) | 8.9 | 0.20 | 0.30 |

$$\left.\frac{1}{\tau_s^{\mathrm{DP}}}\right|_{D,\mathrm{ch}} \approx \frac{64\sqrt{3\pi^3}}{35\sqrt{2}} \frac{(\alpha_c m_c c)^2 \sqrt{a_B^3 n}}{\hbar^5 E_g N_{\mathrm{disl}}} \varepsilon_F^4, \tag{22}$$

and for a nondegenerate electron gas

$$\left.\frac{1}{\tau_s^{\mathrm{DP}}}\right|_{\mathrm{ND,ch}} \approx \frac{3\times 2^{10}}{7\pi^2} \frac{(\alpha_c m_c c)^2 \sqrt{a_B^3 n^\star}}{\hbar^5 E_g N_{\mathrm{disl}}} (kT)^4. \tag{23}$$

### B. Interference effects

For spin scattering from the strain and charge-fields of the *same* dislocation, there is no interference, since the electron being scattered will experience no path difference. The scattering potentials add in such a case due to simultaneous scattering from both fields, and Matheissen's rule is applicable for finding the combined scattering rate. However, for scattering from different dislocations, interference effects need to be considered. Since this work considers a *dilute* distribution of randomly placed dislocations in the semiconductor, it is safe to assume that the individual uncorrelated phase contributions from the two potentials from different dislocations average to zero, similar to a random phase approximation.[25] For example, at the highest dislocation density we consider $(10^{10}/\mathrm{cm}^2)$, there is on an average one dislocation for every square area of side 1000 Å. The interaction of scattering potentials from different dislocations placed far apart is indeed weak, and even weaker when screening is taken into account. This justifies ignoring interference effects in evaluating spin scattering rates.

## V. DISCUSSION AND APPLICATION

Before describing the results, some qualitative observations of the derived spin scattering rates are presented. Experimental evidence shows that in the absence of an external magnetic field, spin scattering by the EY mechanism due to defects (ionized impurities) dominates the spin-scattering rate at the lowest temperatures ($T \leqslant 20$ K).[15] At higher temperatures, DP mechanism dominates.[11] This behavior is also expected for dislocation scattering.

From the results for a nondegenerate electron population, dislocation strain scattering has a $\tau_s \sim (TN_{\mathrm{disl}})^{-1}$ dependence for the EY mechanism and a $\tau_s \sim n^\star/(TN_{\mathrm{disl}})$ dependence for charged core scattering. Strong screening (large $n^\star$) is expected to make spin scattering less susceptible to charged core scattering. EY scattering becomes more severe as the density of dislocations increases, as well as when the carriers become more energetic, i.e., at high temperatures. Similarly, spin scattering time by dislocation strain fields by the DP mechanism has a $\tau_s \sim N_{\mathrm{disl}}/T^4$ dependence, and a $\tau_s \sim N_{\mathrm{disl}}/T^4\sqrt{n^\star}$ dependence for charge scattering. DP scattering becomes less severe with increasing dislocation density, but is very strongly dependent on temperature; it is evident that DP scattering is expected to dominate spin scattering times at high temperatures (including room temperature). Similar observations can be made for degenerate electron distributions.

The derived spin-scattering rates due to dislocations are applied to study the effects on spin transport in three representative direct-gap III-V semiconductors InAs, GaAs, and GaN. The material properties that are relevant to the calculation are listed in Table I. Note that the SO-splitting term $\Delta$ is rather small for GaN, as expected for a wide bandgap semiconductor. Note also the general trend that for small $\Delta$, $\Gamma \sim \Delta^2/E_g^2$, and $\alpha_c \sim \Delta/E_g$, and the spin scattering times $\tau_s^{\mathrm{EY}} \sim E_g^4/\Delta^2$ and $\tau_s^{\mathrm{DP}} \sim E_g^3/\Delta^2$. This indicates a rather strong dependence of spin scattering times on the band structure—a wide bandgap semiconductor with a small spin-orbit coupling is very resistant to spin scattering.

Figure 2 shows a plot of the dislocation-scattering limited spin relaxation time for a non-degenerate electron population of concentration $n_{3d}=3.5\times 10^{16}/\mathrm{cm}^2$ in bulk GaN, GaAs, and InAs. Each of the semiconductor crystals is assumed to be infected with a threading edge dislocation density of $N_{\mathrm{disl}}=5\times 10^8/\mathrm{cm}^2$. The parameters used for the calculation

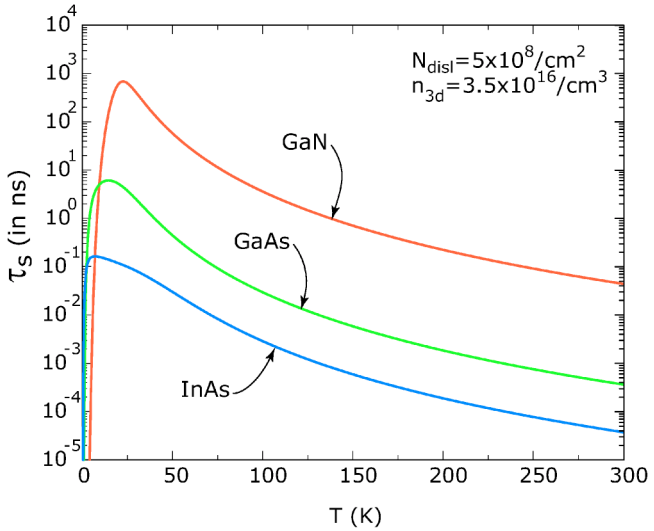


FIG. 2. Spin-scattering time due to dislocations calculated for the nondegenerate regime. The electron concentration and dislocation density is assumed constant. The room-temperature spin-scattering rate for GaN is in good agreement with the experimentally measured value (Ref. 8). Also note that spin scattering by dislocations is very weak for wide-gap semiconductors with small spin-orbit coupling.

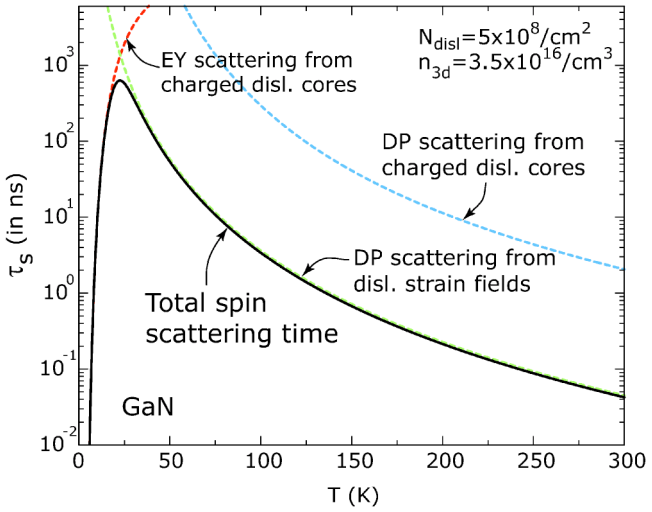


FIG. 3. Relative strengths of individual dislocation spin-scattering mechanisms for GaN. Note that for spintronic devices operating near room-temperature, DP scattering from the strain fields surrounding dislocations dominates spin transport.

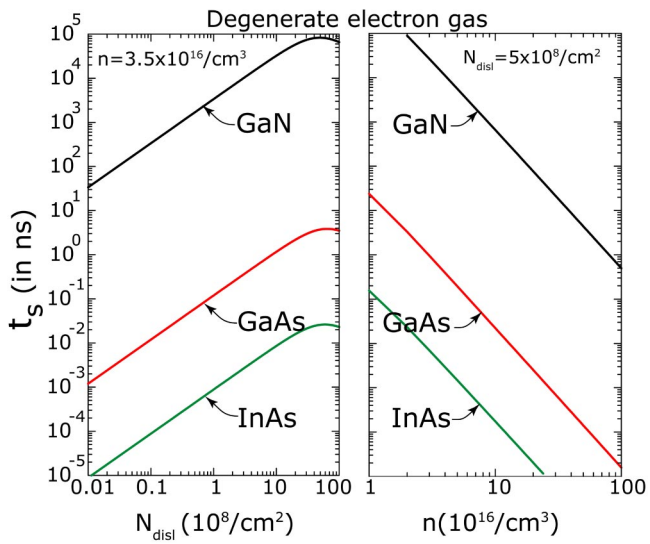


FIG. 4. Spin-scattering times by dislocations for degenerate electron populations for the three semiconductors. Note that in the regime covered, the larger the dislocation density, the less is the spin scattering for the same carrier concentration, highlighting the importance of the DP scattering mechanism. For the same dislocation density, spin-scattering becomes more efficient with increasing carrier density. Temperature does not play a role for the ideal degenerate carrier distribution considered.

are $|\mathbf{b_e}|=a_0$, and the line charge density $c=a_0$ for GaAs and InAs and $c=c_0$ for GaN. For the same dislocation densities and similar carrier concentrations, spin transport in GaN is much more resistant to dislocation scattering than in GaAs or InAs. Figure 3 shows a breakup of the different scattering mechanisms that determine the spin-scattering rates for GaN at each temperature. At the lowest temperatures, EY-scattering from charged dislocation cores is found to be most effective in determining the spin-scattering rates. At temperatures $T \geqslant 20$ K, spin scattering occurs predominantly by the strain fields surrounding dislocations by the DP mechanism. Note that EY scattering from dislocation strain fields and DP scattering from charged dislocation cores are relatively ineffective processes.

The dislocation scattering-limited spin scattering times for degenerate electron distributions as functions of dislocation densities and carrier concentrations is shown in Fig. 4. The dominance of DP scattering is highlighted by the increase of spin-scattering time with increasing dislocation density. For the same reasons, as the carrier density increases, dislocation potentials are better screened, the momentum scattering rate decreases, and as a result, DP scattering rate increases. Note here that any experimentally measured spin-scattering time depends upon the momentum scattering times in the form $\tau_s^{\mathrm{EY}} \sim \tau_1$ and $\tau_s^{\mathrm{DP}} \sim 1/\tau_1$, where $\tau_1$ is the momentum scattering time due to *all* scattering mechanisms. By Matheissen's rule, $\tau_1$ is determined by the *strongest* scattering mechanism. At very low dislocation densities, $\tau_1$ is determined by either phonon scattering or inonized impurity scattering, and dislocations would not play a part in spin relaxation. Figure 4 should be understood in that light—it shows the spin scattering time due to dislocations alone.

*Comparison with experimental data*. A comparison with experimental observations is now presented. Beschoten *et al.*[8] have reported $\tau_s \approx 20$ ns as $T=5$ K ($n \approx 3.5\times 10^{16}/\mathrm{cm}^3$ and $N_{\mathrm{disl}} \approx 5\times 10^8/\mathrm{cm}^2$), and $\tau_s \approx 35$ ps at $T \approx 300$ K for a GaN sample with $n \approx 1\times 10^{17}/\mathrm{cm}^3$ and $N_{\mathrm{disl}} \approx 5\times 10^8/\mathrm{cm}^2$. They mention the possibility of dislocation scattering being benign to spin relaxation, enabling surprisingly long spin memory in the material in spite of the many orders of magnitude larger dislocation density. The same carrier and dislocation densities as in the sample used by Beschoten *et al.* in their experimental work is used for GaN, GaAs, and InAs for illustrating the dependence of dislocation spin scattering on the bandgap and spin-orbit splitting of the semiconductors.

The calculated spin-scattering time ($\tau_s \approx 43$ ps) for GaN ($n \approx 1\times 10^{17}/\mathrm{cm}^3$) is in reasonably good agreement at room temperature with the experimental data ($\tau_s \approx 35$ ps).[8] At lower temperatures, other scattering mechanisms (e.g., ionized impurity scattering) probably dominate the measured lifetimes, which are much shorter than what would be expected from dislocation scattering. Krishnamurthy *et al.* calculated[3] spin-scattering times from all scattering mechanisms (phonons, ionized impurities) *excluding* dislocations for GaN to be $\tau_s \approx 100$ ns at 300 K, which is much larger than the experimental value. This work offers an explanation for the experimentally observed value by considering dislocation scattering. DP scattering by the strain fields surrounding dislocations is identified to be the primary spin-scattering mechanism at and around room temperature.

Note also that for bulk InAs grown on GaAs with a carrier concentration $n_{3d} \approx 2\times 10^{16}/\mathrm{cm}^3 - \tau_s \sim 10-20$ ps was reported by Boggess *et al.*[26] However, they do not discuss the individual scattering mechanisms in their work. Due to the scarcity of *systematic* studies of the effect of dislocation scattering on spin transport in InAs and GaAs materials, experimental data is not discussed any further in this work. As such studies are carried out with lattice-mismatched materials with high dislocation densities, the theory presented here

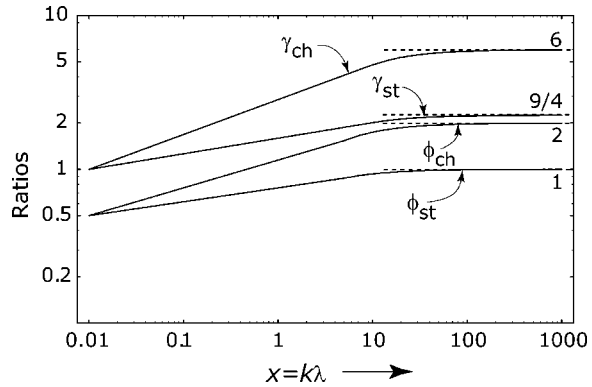


FIG. 5. *Exact* ratios $\Phi_{st}, \Phi_{ch}$ and $\gamma_{st}, \gamma_{ch}$, that relate the spin scattering rates to the momentum scattering rates, and their asymptotic values as a function of the dimensionless quantity $x = k\lambda$. $\Phi$ terms are due to the Elliott-Yafet scattering mechanism, and $\gamma$ terms due to the D'Yakonov-Perel scattering mechanism.

may be used as a guideline for interpreting trends and the effect of dislocation scattering.

## VI. CONCLUSIONS

An important observation is that at high temperatures, since DP mechanism dominates, a sample with more dislocations will have a *longer* spin scattering time due to dislocations. This might prove to be beneficial for achieving spin transport over long distances. A wide bandgap semiconductor (with small SO splitting, such as GaN) with a fair amount of dislocations can be deposited on a narrow bandgap semiconductor, and still retain large spin lifetimes. This counterintuitive result may prove to be especially advantageous for the design of lattice-mismatched heterostructure spintronic devices for spin communication over long distances. Note that if the dislocation density becomes too large, EY mechanism may start playing an important role at higher temperatures. In addition, space-charge regions around charged dislocations can overlap, leading to reduction of free carriers, and to carrier localization as well.[23,24]

So there exists a window of dislocation densities within which spin transport at normal operating temperatures for devices is improved by the controlled introduction of dislocations. There should be no confusion about the *total* spin-scattering rate due to phonons, ionized dopants, and other defects; for any given semiconductor, if one prevents dislocations altogether, one gets the least spin scattering. However, if one wants to take advantage of the small spin scattering in a wide bandgap spin-transport layer in conjunction with a narrow-gap spin-control layer, dislocations are inevitable. Then, it is better to have a controllably large dislocation density in the spin-transport layer for large room-temperature spin lifetimes. Though any form of scattering is a bane for spin transport, the relative insensitivity of dislocation scattering for wide-bandgap semiconductors might prove to be a boon, leading to novel design paradigms for spintronic devices.

## APPENDIX

The crucial link between the momentum and spin-scattering rates by both the EY and DP spin scattering mechanisms are the ratios $\Phi$ and $\gamma$ defined earlier. Here, the *exact* forms of the ratios for spin scattering by dislocations as functions of the dimensionless quantity $x = k\lambda$ are listed.

For the EY mechanism, the factor $\Phi_{st}$ for scattering by strain fields of dislocations is found to be

$$\Phi_{st}(x) = \frac{y(1 + x^2 - y)}{x^2(y - 1)}, \tag{A1}$$

which has an asymptotic value $\Phi_{st}(x \to \infty) = 1$. Here $y = \sqrt{1 + 2x^2}$. Similarly, the factor $\gamma_3$ for DP scattering by the strain field is

$$\gamma_{st}(x) = \frac{3x^4(3y - 8) - 30x^2 + 10(y^3 - 1)}{4x^4(y - 1)}, \tag{A2}$$

with an asymptotic behavior $\gamma_{st}(x \to \infty) = 9/4$.

For the Coulombic charge field around dislocation, the EY factor is found to be

$$\Phi_{ch}(x) = \frac{y^2(1 + x^2 - y)}{x^4}. \tag{A3}$$

The asymptotic value is $\Phi_{ch}(x \to \infty) = 2$. Similarly, the DP factor is

$$\gamma_{ch}(x) = \frac{2x^6 + 5x^4y^2 - 10y^3(1 + x^2) + 10y^4}{2x^6}, \tag{A4}$$

with an asymptotic value of $\gamma_{ch}(x \to \infty) = 6$. The dependence of the four spin-scattering factors on the dimensionless quantity $k\lambda$, with the mentioned asymptotic values is shown in Fig. 5.

*Electronic mail: djena@nd.edu

[1] S. Datta and B. Das, Appl. Phys. Lett. **56**, 665 (1990).

[2] Spin injection *across* junctions is a pressing problem currently for realization of spintronic devices, and has been the topic of many review papers [see, for example, I. Zutic, J. Fabian, and S. D. Sarma, Rev. Mod. Phys. **76**, 323 (2004)]. This work concentrates on dislocation scattering exclusively, and does not address that issue.

[3] S. Krishnamurthy, M. Schilfgaarde, and N. Newman, Appl. Phys. Lett. **83**, 1761 (2003).

[4] P. H. Song and K. W. Kim, Phys. Rev. B **66**, 035207 (2002).

[5] J. M. Kikkawa and D. D. Awschalom, Phys. Rev. Lett. **80**, 4313 (1998).

[6] V. M. Zholkevskii and G. A. Denisenko, Phys. Solid State **43**, 1905 (2001).

[7] R. M. Stroud *et al.*, Phys. Rev. Lett. **89**, 166602 (2002).

[8] B. Beschoten *et al.*, Phys. Rev. B **63**, 121202(R) (2001).

[9] S. DasSarma and F. Stern, Phys. Rev. B **32**, 8442 (1985).

[10] D. Jena and U. K. Mishra, Phys. Rev. B **66**, 241307(R) (2002).
[11] G. E. Pikus and A. N. Titkov, in *Optical Orientation* (North Holland, Amsterdam, 1986).
[12] G. Dresselhaus, Phys. Rev. **100**, 580 (1955).
[13] R. J. Elliott, Phys. Rev. **96**, 266 (1954).
[14] Y. Yafet, in *Solid State Physics*, edited by F. Seitz and D. Turnbull (Academic, New York), Vol. 14.
[15] J.-N. Chazalviel, Phys. Rev. B **11**, 1555 (1975).
[16] V. F. Gantmakher and Y. B. Levinson, in *Carrier Scattering in Metals and Semiconductors* (North Holland, Elsevier, 1987).
[17] M. I. D'Yakonov and V. I. Perel, Sov. Phys. Solid State **13**, 3023 (1971).
[18] C. Shi, P. M. Asbeck, and E. T. Yu, Appl. Phys. Lett. **74**, 573 (1999).
[19] D. Jena and U. K. Mishra, Appl. Phys. Lett. **80**, 64 (2002).
[20] K. Seeger, *Semiconductor Physics, An Introduction* (Springer Verlag, Berlin, 1999), p. 222.
[21] B. Pödör, Phys. Status Solidi **16**, K167 (1966).
[22] D. C. Look and J. R. Sizelove, Phys. Rev. Lett. **82**, 1237 (1999).
[23] W. T. Read, Philos. Mag. **45**, 775 (1954).
[24] N. G. Weimann *et al.*, J. Appl. Phys. **83**, 3656 (1998).
[25] D. K. Ferry and S. M. Goodnick, *Transport in Nanostructures* (Cambridge, United Kingdom, 1997), p. 70.
[26] T. F. Boggess *et al.*, Appl. Phys. Lett. **77**, 1333 (2000).